MINIREVIEW

Check for updates

Machine-enabled inverse design of inorganic solid materials: promises and challenges

Juhwan Noh, [ID] Geun Ho Gu, Sungwon Kim and Yousung Jung [ID] *

Developing high-performance advanced materials requires a deeper insight and search into the chemical space. Until recently, exploration of materials space using chemical intuitions built upon existing materials has been the general strategy, but this direct design approach is often time and resource consuming and poses a significant bottleneck to solve the materials challenges of future sustainability in a timely manner. To accelerate this conventional design process, inverse design, which outputs materials with pre-defined target properties, has emerged as a significant materials informatics platform in recent years by leveraging hidden knowledge obtained from materials data. Here, we summarize the latest progress in machine-enabled inverse materials design categorized into three strategies: high-throughput virtual screening, global optimization, and generative models. We analyze challenges for each approach and discuss gaps to be bridged for further accelerated and rational data-driven materials design.

1 Introduction

Technical demands for developing more advanced materials are continuing to increase, and developing improved functional materials necessitates going far beyond the known materials and digging deep into the chemical space.[1] One of the fundamental goals of materials science is to learn structure–property relationships and from them to discover novel materials with desired functionalities. In traditional approaches, a candidate material is specified first using intuition or by slightly changing the existing materials, and their properties are scrutinized experimentally or computationally, and the process is repeated until one finds reasonable improvements to known materials (*i.e.* incremental improvement from the firstly discovered materials).[2] This conventional approach is driven heavily by human experts' knowledge and hence the results vary person to person and can also be slow. Materials informatics deals with the use of data, informatics, and machine learning (ML, complementary to experts' intuitions) to establish structure–property relationships for materials and make a new functional discovery at a significantly accelerated rate. In materials informatics, human experts' knowledge is thus either incorporated into algorithms and/or completely replaced by data.

There are two mapping directions (*i.e.* forward and inverse) in materials informatics. In a forward mapping, one essentially aims to predict the properties of materials using materials structures as input, encoded in various ways such as simple attributes of constituent atoms, compositions, structures in

graph forms, *etc.* In an inverse mapping, by contrast, one defines the desired properties first and attempts to find materials with such properties in an inverse manner using mathematical algorithms and automations. While forward mapping mainly deals with property prediction given structures, inverse mapping focuses on the "design" aspect of materials informatics towards target properties. For effective inverse design, therefore, one needs (1) efficient methods to explore the vast chemical space towards the target region ("exploration"), and (2) fast and accurate methods to predict the properties of a candidate material along with chemical space exploration ("evaluation").

The purpose of this mini-review is to survey exciting new developments of methods to perform inverse design by "exploring" the chemical space effectively towards the target region. We will particularly highlight the design of inorganic solid-state materials since there are excellent recent review articles in the literature for the molecular version of inverse design.[3,4] To structure this review, we categorize the inverse design strategies of inorganic crystals as summarized in Fig. 1, namely, high-throughput virtual screening (HTVS), global optimization (GO), and generative ML models (GM), largely borrowing the classification of Sanchez-Lengeling and Aspuru-Guzik[3] and Butler *et al.*[5] Among them, HTVS may be regarded as an extended version of the direct approach since it goes through the library and evaluates its function one by one, but the data-driven nature of the automated, extensive, and accelerated search in the functional space makes it potentially included in the inverse design strategy.[6]

One of the drawbacks of HTVS, however, is that, the search is limited by the user-selected library (either the experimental database or substituted computational database) and experts'

Department of Chemical and Biomolecular Engineering, Korea Advanced Institute of Science and Technology (KAIST), 291, Daehak-ro, Yuseong-gu, Daejeon 34141, Republic of Korea. E-mail: ysjn@kaist.ac.kr
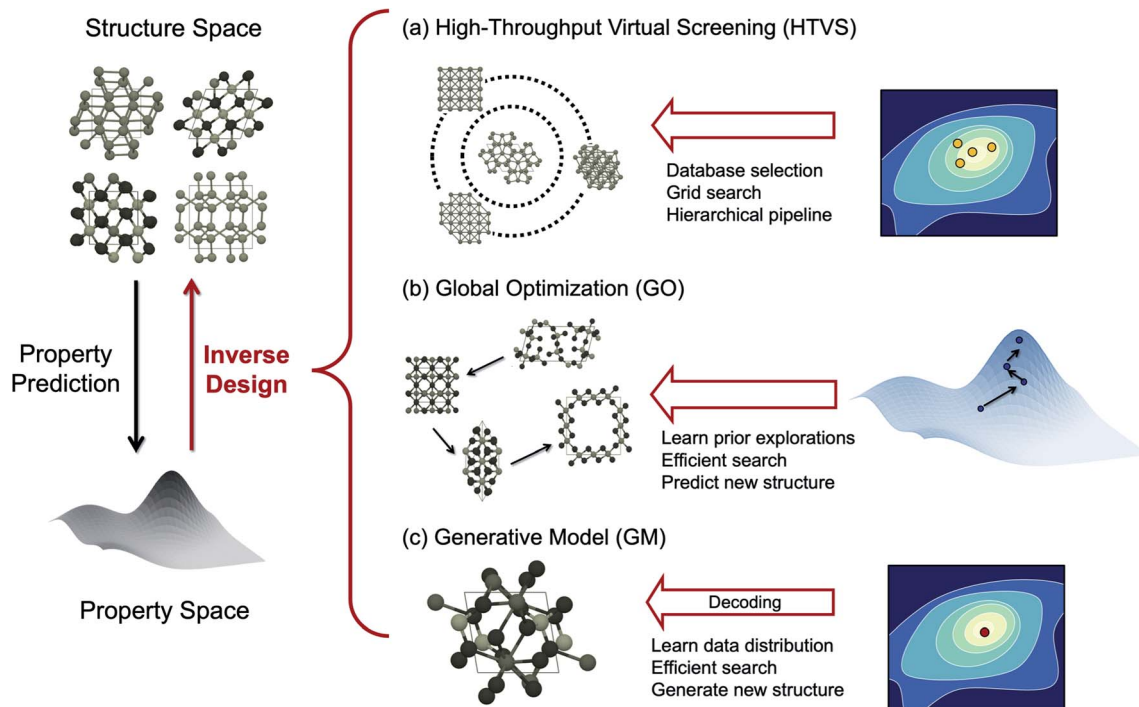
Fig. 1 Scheme of materials informatics learning the structure–property relationships of materials either for property predictions or designing materials with target properties depending on the mapping direction. Inverse design is further categorized into (a) high throughput virtual screening (HTVS), (b) global optimization (GO), and (c) generative model (GM), depending on the strategy how each approach explores the chemical space.

(sometimes biased) intuitions are still involved in selecting the database, and thus potentially high-performing materials that are not in the library can be missed out. Also, since the screening is run over the database blindly without any preferred directions to search, the efficiency can be low in HTVS. One way to expedite the brute-force search toward the optimal material is to perform global optimization (GO) in the chemical space. In evolutionary algorithms (EAs), one form of GO, for example, mutations and crossover allow effective visits of various local minima by leveraging the previous histories of configurational visits, and therefore can generally be more efficient and also go beyond the chemical space defined by known materials and their structural motifs unlike HTVS.[7]

The data-driven GM is another promising inverse design strategy.[3] The GM is a probabilistic ML model that can generate new data from the continuous vector space learned from the prior knowledge on dataset distribution.[3,21] The key advantage of GMs is their ability to generate unseen materials with target properties in the gap between the existing materials by learning their distribution in the continuous space. While both the EA and GM can generate completely new materials not in the existing database, they differ by the way each approach utilizes data. The EA learns the geometric landscape of the functionality manifold (energy and properties) implicitly as the iteration evolves, while the GM learns the distribution of the whole target functional space during training in an implicit (*i.e.* adversarial learning) or explicit (*i.e.* variational inference) manner.

Below we summarize the current status and successful examples of these three main strategies (HTVS, GO, and GM) of the data-driven inorganic inverse design approach. We also discuss several challenges for the practical application of accelerated inverse materials design and also offer some promising future directions.

2 Inverse design strategy

2.1 High-throughput virtual screening (HTVS)

The computational HTVS is a widely used discovery strategy in the field. Usual computational HTVS involves three steps: (1) defining the screening scope, (2) first principles-based (or sometimes empirical models) computational screening and (3) experimental verifications for the proposed candidates. Defining the screening scope involves field experts' heuristics, and the success of the screening highly depends on this step as the scope must contain promising materials, but it should not be so wide that the computational HTVS becomes too expensive. To save cost, computational funnels are often used where cheaper methods or easier-to-compute properties are used as initial filtering and more sophisticated methods or properties hierarchically narrow down candidates for a pool of final selections. Density functional theory (DFT) is usually used for the computational HTVS, but ML models for property predictions further accelerate the screening process significantly (evaluation aspect of materials informatics in Fig. 1a). For experimental verifications, the key step in the

computational HTVS, high-throughput experimental methods such as sputtering can greatly help to survey a wide variety of synthesis conditions and activity.[8] If activity is observed, more expensive characterization techniques are used to confirm the crystals.

Using the computational HTVS going through the existing database, Reed and co-workers[9] discovered 21 new Li-solid electrolyte materials by screening 12 831 Li-containing materials in the materials project (MP).[10] Singh and co-workers[11] newly identified 43 photocatalysts for CO_2 conversion through the theory/experiment combined screening framework for 68 860 materials available in MP. However, as discussed above, moving beyond the known materials is critical, and to address it, a new functional photoanode material has been discovered by enumerating hypothetical materials by substituting elements to the existing crystals.[12] Recently, data mining-[13] and deep learning-based[14] algorithms for elemental substitution are proposed to effectively search through the existing crystal templates, and Sun et al.[15] discovered a large number of metal nitrides using the data-mined elemental substitution algorithm which accelerated the experimental discovery of nitrides by a factor of 2 compared to the average rate of discovery listed on the inorganic crystal structure database, ICSD.[16,17]

Despite those successful results, the large computational cost for property evaluation using DFT calculations is still a main bottleneck in the computational HTVS, and to overcome the latter challenge, ML-aided property prediction has begun to be implemented (see Table 1 and ref. 18 and 19 for an extensive review on ML used in property predictions). Herein, we mainly focus on ML models predicting the stability of crystal structures since the stability represented by the formation energy is a widely used quantity, though crude, to approximate synthesizability in many materials designs.

Non-structural descriptor-based ML models have been proposed.[20,22] For example, Meredig et al.[22] proposed a formation energy prediction model for ~15 000 materials existing in the ICSD[16,17] using both data-driven heuristics utilizing the composition-weighted average of corresponding binary compound formation energies (MAE = 0.12 eV per atom) and ensembles of decision trees which take average atomic properties of constituent elements as input (MAE = 0.16 eV per atom). The proposed models were used to explore ~1.6 million ternary compounds, and 4500 new stable materials were identified with the energy above convex hull ≤100 meV per atom. With the latter examples considering compositional information only, Seko et al.[23] have shown that the inclusion of structural information such as radial distribution function could further improve the prediction accuracy significantly from RMSE = 0.249 to 0.045 eV per atom for a cohesive energy of 18 000 inorganic compounds with kernel ridge regression.

ML models that encode the structural information of crystals for the prediction of energies and properties have also been proposed. Notably, Xie et al.[24] proposed the symmetry invariant crystal graph convolutional neural network (CGCNN) to encode periodic crystal structures which showed very encouraging predictions for various properties including formation energies (MAE = 0.039 eV per atom) and band gaps (MAE = 0.388 eV). An improved version of CGCNN was also proposed by incorporating explicit 3-body correlations of neighboring atoms and applied to identify stable compounds out of 132 600 structures obtained by tertiary elemental substitution of $ThCr_2Si_2$-structure prototype.[25] Lately, the graph-based universal ML model that can treat both molecules and periodic crystals was proposed and demonstrated highly competitive accuracy across a wide range of 15–20 molecular and materials properties.[24–27]

Table 1 List of representations used for inverse design (HTVS and GM) of inorganic solid materials. Invertibility is the existence of inverse transform from representation to crystal structure, and invariance refers to the invariance of representation to translation, rotation, and unit cell repeat. The models and target applications are also listed for each reference

Representation	Invertibility	Invariance	Model	Application
Supervised learning (property prediction in HTVS)				
Atomic properties[56,57]	No	Yes	SVR	Predicting melting temperature, bulk and shear modulus, bandgap
Crystal site-based representation[20]	Yes	Yes	KRR	Predicting formation energy of ABC_2D_6 elpasolite structures
Average atomic properties[22]	No	Yes	Ensembles of decision trees	Predicting the formation energy of inorganic crystal structures
Voronoi-tessellation-based representation[58]	No	Yes	Random forest	Predicting the formation energy of quaternary Heusler compounds
Crystal graph[24]	No	Yes	GCNN	Predicting formation enthalpy of inorganic compounds
Unsupervised learning (GM)				
3D atomic density[59,79]	Yes	No	VAE	Generation of inorganic crystals
3D atomic density and energy grid shape[60]	Yes	No	GAN	Generation of porous materials
Lattice site descriptor[61]	Yes	No	GAN	Generation of graphene/BN-mixed lattice structures
Unit cell vectors and coordinates[36,62]	Yes	No	GAN	Generation of inorganic crystals

While looking promising, one of the more practical challenges of ML-aided HTVS for crystals is that some property data is often limited in size to expect good predictive accuracy for model training across different chemistries.[26,28] (A more general comparison between the inorganic crystal dataset and organic molecule database is discussed in more detail in a later section. See also Fig. 4) To address this small dataset size, algorithms such as transfer learning (*i.e.* using pre-trained parameters before training the model on the small-size of the database)[29] and active learning (*i.e.* effectively sampling the training set from the whole database)[30,31] could help. For example, one may build the ML model to predict computationally more difficult properties (*e.g.* band gap and bulk modulus) using model parameters trained on a relatively simple property (*e.g.* formation energy),[26] and this would help prevent overfitting driven by using a smaller dataset for difficult properties.
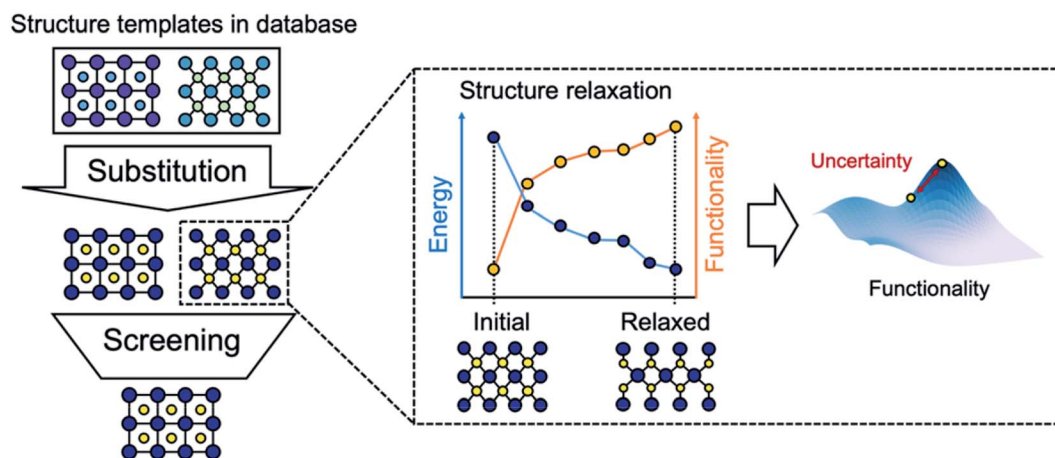
Furthermore, it is important to note that most current ML models to predict energies for crystals can only evaluate energies on relaxed structures, but cannot (or have not been shown to) calculate forces. Thus, when elemental substitution (which requires geometry relaxation) is used to expand the search space, one cannot use aforementioned ML models and still must perform costly DFT structure relaxations for every substituted structure as shown in Fig. 2a. To address this, data-driven interatomic potential models[32–34] that can compute forces and construct a continuous potential energy surface are particularly promising, although they have not been widely used for HTVS of crystals yet since potentials are often developed for particular systems and so not applicable for the screening of widely varying systems. Or, still using the energy-only ML model but quantifying uncertainty caused by using unrelaxed structures could be an alternative way to increase the practical efficiency of HTVS.[35] In addition, since the substitution-based enumeration limits the structural diversity of the dataset, generative models which will be discussed in detail below can effectively expand the diversity by sampling the hidden portion of the chemical space[36] as shown in Fig. 2b.

2.2 Global optimization (GO)

Global optimization, including, but not limited to, quasi random search, simulated annealing, minima hopping, genetic algorithm, and particle swarm optimization, is an algorithm to find an optimal solution of target objective function, and thus it
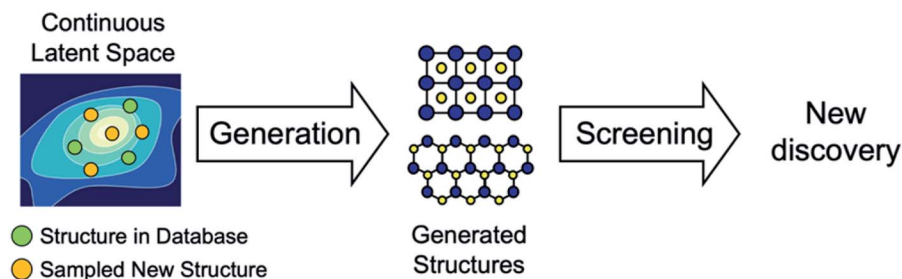

Fig. 2 ML–aided HTVS. (a) In practical HTVS based on elemental substitution, newly substituted materials require costly DFT structure relaxations before evaluating functionality. As a way to bypass structure relaxations, property prediction ML models can be augmented with uncertainty quantification incurred by the use of unrelaxed geometry. (b) Generative models can be used to produce new hypothetical crystal structures for HTVS that go beyond the existing structural motifs.

can be used for various inverse design problems.[37] Many of these applications involve some form of crystal structure predictions. One of the earlier examples of GO applied to materials science is the work of Franceschetti and Zunger[38] in which they used a simulated annealing approach to inversely design the optimal atomic configuration of the superlattice of $Al_xGa_{1-x}As$ alloys having the largest optical bandgap. Also, Doll *et al.*[39] used a simulated annealing approach combined with *ab initio* calculations to predict the structure of boron nitride where various types of energetically favorable structures (*e.g.* layered structure, the wurtzite and zinc blende structure, β-BeO type and so on) were discovered showing the effectiveness of simulated annealing for crystal structure prediction. Random structure search, often constrained by a few chemical rules, is one of the simplest yet successful search strategies to find new phases of crystals, and Pickard and Needs combined it with first-principles calculations to predict the stable high-pressure phases of silane, for example.[97]

Amsler and Goedecker[40] proposed the minima hopping method to discover new crystal structures by adapting the softening process which modifies initial molecular dynamic velocities to improve the search efficiency. The latter minima hopping approach was extended to design transition metal alloy-based magnetic materials (FeCr, FeMn, FeCo and FeNi) by combining with additional steps evaluating magnetic properties (*i.e.* magnetization and magnetic anisotropy energy).[41] FeCr and FeMn were predicted as soft-magnetic materials while FeCo and FeNi were predicted as hard-magnetic materials.

Evolutionary algorithms use strategies inspired by biological evolution, such as reproduction, mutation, recombination, and selection, and they can be used to find new crystal structures with optimized properties. The properties to optimize can be stability only (called convex hull optimization) or both stability and desired chemical properties (called Pareto or multi-objective optimization, see ref. 37 for more technical details). Two popular approaches include the Oganov-Glass evolutionary algorithm[42] and Wang's version of particle swarm optimization.[43] While the detailed updating process of each algorithm is different,[37] the two key steps are commonly shared: (1) generating a population consisting of randomly initialized atomic configurations and (2) updating the population after evaluating stability (or/and property) of each configuration existing in the population, using DFT calculations or ML-based methods for an accelerated search. One of the major advantages of EA-based models is their capability to generate completely new materials beyond existing databases and chemical intuitions.

For convex hull optimization, Kruglov *et al.*[44] proposed new stable uranium polyhydrides (U_xH_y) as potential high-temperature superconductors. Zhu *et al.*[45] systematically investigated the (V,Nb)-(Fe,Ru,Os)-(As,Sb,Bi) family of half-Heusler compounds where 6 compounds were identified as stable and entirely new structures, and 5 of them were experimentally verified as stable with a half-Heusler crystal structure. Multi-objective optimization led to the inverse discovery of new crystal structures with various properties in addition to stability. Zhang *et al.*[46] proposed 24 promising electrides with an optimal degree of interstitial electron localization where 18 candidates

were experimentally synthesized that have not been proposed as electrides previously. Xiang *et al.*[47] discovered a cubic Si_{20} phase, a potential candidate for thin-film solar cells, with a quasi-direct band gap of 1.55 eV. Bedghiou *et al.*[48] discovered new structures of rutile-TiO_2 with the lowest direct band gap of 0.26 eV under (ultra)high pressure conditions (*i.e.* up to 300 GPa) by simultaneously optimizing the stability and band gap during the evolutionary algorithm.

As in HTVS, the large computational cost for property evaluations is a major bottleneck (99% of the entire cost[49]) in EA (or GO in general) and ML models can greatly help. Of course, the same property prediction ML models or interatomic potentials described in HTVS can also be used in EAs, as shown in Fig. 3a. In specific examples, Jennings *et al.*[50] proposed an ML-based genetic algorithm framework by adapting on-the-fly a Gaussian process regression model to rapidly predict target properties (energy in this case). Here, for Pt_xAu_{147-x} alloy nanoparticles, the genetic algorithm was shown to reduce the number of configurational visits (or DFT energy calculations) from 10^{44} (brute force combinatorial possibilities) to 16 000, and with the Gaussian process model described above, the required DFT calculations were further reduced to 300, representing 50-fold reduction in cost due to ML. Avery *et al.*[51] constructed a bulk modulus prediction ML model, trained with the database existing in the Automatic FLOW (AFLOW)[52] library, and used it to predict new 43 superhard carbon-phases in their EA-based materials design. Podryabinkin *et al.*[49] used a moment tensor potential-based ML interatomic potential to replace expensive DFT structure relaxations in their crystal structure prediction of carbon and boron allotropes using EAs. The authors were able to find all the main allotropes as well as to find a hitherto unknown 54-atom structure of boron with substantially low cost.

Since most EA-based methods need a fixed chemical composition as input, one often needs to try many different compositions or requires experts' guess for the initial composition. To address this computational difficulty of searching through a large composition space, the recently proposed ML-based[53] and tensor decomposition-based[54] chemical composition recommendation models are noteworthy since those models could provide promising unknown chemical compositions from prior knowledge of experimentally reported chemical composition. Furthermore, Halder *et al.*[55] combined the classification ML model with EAs, in which the classification model selected potentially promising compositions that would go into the EA-based crystal structure prediction as shown in Fig. 3b. The authors applied the method to find new magnetic double perovskites (DPs). They first used the random forest to select elemental compositions in $A_2BB'O_6$ (A = Ca/Sr/Ba, B/B' = transition metals) as potentially stable DPs (finding 33 compounds out of 412 unexplored compositions), and using EA and DFT calculations they subsequently identified new 21 DPs with various magnetic and electronic properties.

2.3 Generative models (GM)

The generative model is an unsupervised learning that encodes the high-dimensional materials chemical space into the

(a) ML-accelerated structure relaxation and property prediction

Evolutionary algorithm (EA)
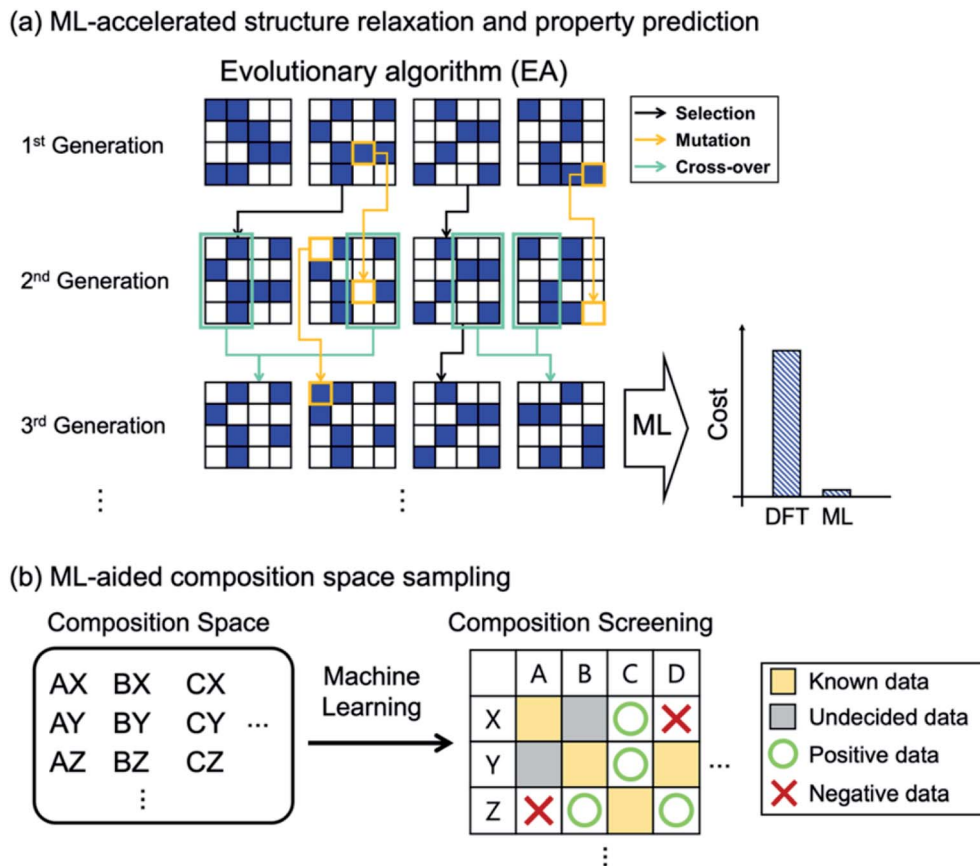

## (b) ML-aided composition space sampling

Fig. 3 (a) Evolutionary algorithm optimizes materials (or atomic configurations) by using three operations derived from biological evolution. Selection (black arrow) chooses stable materials after evaluating functionality. Mutation (orange arrow) introduces variation in original materials. Crossover (green arrow) mixes two different materials. Along with these operations, materials are optimized to have target functionality. To avoid costly first-principles evaluation of functionality, ML could greatly reduce the computational burden. (b) ML can be used to search through composition space to discriminate positive (*i.e.* promising, green circle) *vs.* negative (*i.e.* unpromising, red cross) cases.

continuous vector space (or latent space) of low dimension, and generates new data using knowledge embedded in the latent space.[3] However, unlike molecular generative models, there are only a few examples on crystal structure generative models due to the following difficulties: (1) invertibility of representations for periodic crystal structures, (2) symmetry invariance for translation, rotation, and unit cell repeat, and (3) low structural diversity (data) per element of inorganic crystal structures compared to the molecular chemical space. The first two issues (invertibility and invariance) correspond to the characteristics of representations (see Table 1) while the third (chemical diversity) is related to the data used for training.

We first note that for organic molecules there are several string-based molecular representations that are symmetry-invariant and invertible as in SMILES[63] and SELFIES,[64] for which many language-based ML models such as RNN,[65] Seq2-Seq,[66] and attention-based Transformer model[67] can be applied.[21,98] Furthermore, graph representation is another popular approach for organic molecules since chemical bonds between atoms in molecules can be explicitly defined and this can allow an inverse mapping from graph to molecular structure. Various implicit and explicit GMs[68–70] have been proposed by adopting a graph convolutional network for organic

molecules.[71] However, in the case of crystal structures, currently there is no explicit rule to convert crystal structures into string-based representations, or *vice versa*. Although graph representation has been proposed with great success on property predictions, there is currently no explicit formulation on decoding the crystal graph back to the 3D crystal structure.

A low structural diversity (or data) per element for the inorganic crystal structure database is another critical bottleneck in establishing GMs (or in fact any ML models) for inorganic solids compared to organic molecules (see Fig. 4). This is because, for organic molecules, only a small number of main group elements can produce an enormous degree of chemical and structural diversity, but for inorganic crystals, the degree of structural diversity per chemical element is relatively low and not well balanced compared to molecules (for example, there are 2506 materials having ICSD-ids in MP that contain iron, but only 760 materials that contain scandium). This low structural diversity could bias the model during the training, and it may not able to generate so meaningful and very different new structures from existing materials. This makes a universal GM for inorganic crystals that covers the entire periodic table quite challenging.
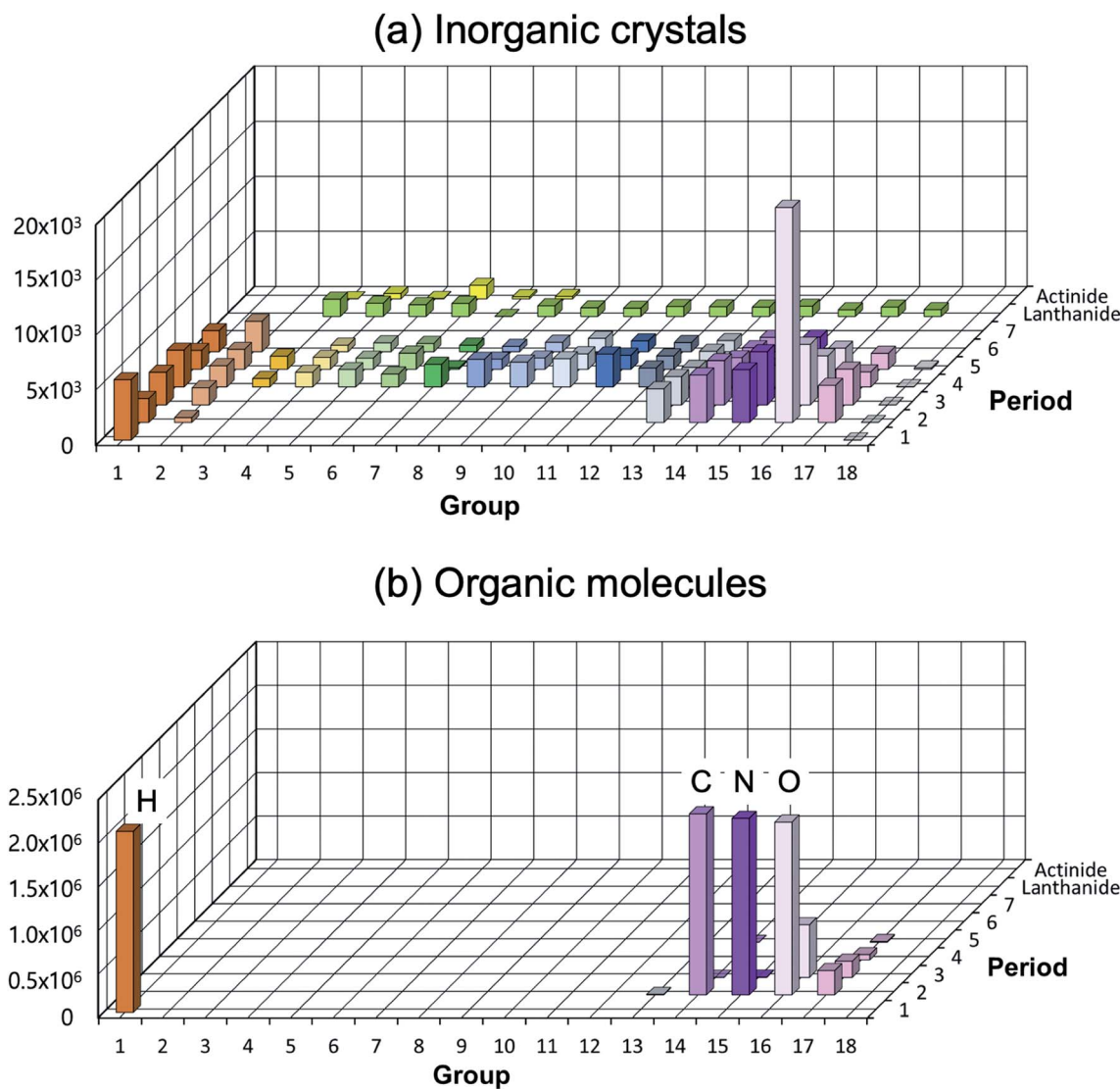
(a) Inorganic crystals

(b) Organic molecules
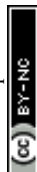
Fig. 4 Distribution of elements existing in the crystal/molecular database. (a) Experimentally reported inorganic materials (# of data = 48 567) taken from MP.[10] They cover most elements in the periodic table (high elemental diversity), but the number of data per element is sparsely populated (low structural diversity). (b) Organic molecules taken from the subset of the ZINC database (# of data = 2 077 407).[72] They cover very limited elements (low elemental diversity), but are densely populated (high structural diversity).

Despite these challenges, there are some promising initial results for inorganic crystal generative models that addressed some of the aforementioned difficulties. Two concepts of GMs have been implemented for solid state materials recently (see Fig. 5a and b): variational autoencoder (VAE)[73] and generative adversarial network (GAN).[74] Here, we note that other generative frameworks (*e.g.* conditional VAE[75]/GAN,[76] AAE,[77] VAE-GAN,[78] *etc.*) derived from the latter two models can be applied depending on target objectives. VAE explicitly regularizes the latent space using known prior distributions such as Gaussian and Bernoulli distribution. Compared to VAE, the GAN implicitly learns the data distribution by iteratively checking the reality of the generated data from the known prior latent space distribution.

Noh *et al.*[59] proposed the first GM for inorganic solid-state materials structures using a 3D atomic image representation

(Fig. 5c). Here, the stability-embedded latent space was constructed under the VAE scheme,[73] and used to generate stable vanadium oxide crystal structures. In particular, due to a low structural diversity of the current inorganic dataset described above, the authors used the virtual V–O binary compound space as a restricted materials space to explore (instead of learning the crystal chemistry across the periodic table). This image-based GM then discovered several new compositions and meta-stable polymorphs of vanadium oxides that have been completely unknown. Hoffmann *et al.*[79] proposed a general purpose encoding-decoding framework for 3D atomic density under the VAE formalism. The model was trained with atomic configurations taken from crystal structures reported in the ICSD[16,17] (which does not impose a constraint in chemical composition), and an additional segmentation network[80] was used to classify the elements information from the generated
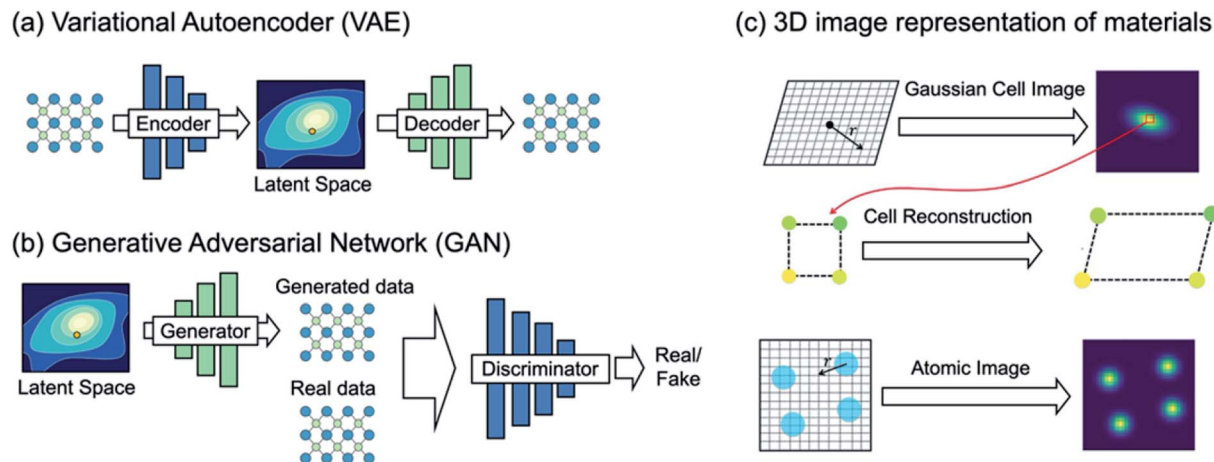
Fig. 5 (a) Variational autoencoder (VAE) learns materials chemical space under the density reconstruction scheme by explicitly constructing the latent space. Each point in the latent space represents a single material, and thus one can directly generate new materials with optimal functionality. (b) Generative adversarial network (GAN), however, learns materials chemical space under the implicit density prediction scheme which iteratively discriminates the reality of the data generated from the latent space. (c) A VAE-based crystal generative framework proposed by Noh et al.[59] using an invertible 3D image representation for the unit cell and basis (adapted with permission from ref. 59 Copyright 2019 Elsevier Inc. Matter).

3D representation. However, we note that the proposed model is focused on generating valid atomic configurations only, and thus an additional network which generates a unit cell associated with the generated atomic configuration would be required to generate new 'materials'.

Despite those promising results, 3D image-based representations have a few limitations, a lack of invariance under symmetry operations and heuristic post-processing to clean up chemical bonds, for example. The former drawback can be approximately addressed by data augmentation,[60] and for example, Kajita et al.[81] showed that 3D representations with data augmentation yielded a reasonable prediction of the various electronic properties of 680 oxide materials. For the latter problem, a representation which does not require heuristic post-processing would be desirable.

Rather than using computationally burdensome 3D representations, Nouira et al.[62] proposed to use unit cell vectors and fractional coordinates as input to generate new ternary hydride structures by learning the structures of binary hydrides inspired by a cross-domain learning strategy. Kim et al.[36] proposed a GAN-based generative framework which uses a similar coordinate-based representation with symmetry invariance addressed with data augmentation and permutation invariance with symmetry operation as described in PointNet,[82] and used it to generate new ternary Mg–Mn–O compounds suitable for photoanode applications. There are also examples in which generative frameworks are used to sample new chemical compositions for inorganic solid materials.[83,84] For these studies, adding concrete structural information would be a desirable further development, similar to the work of Halder et al.,[55] which also highlights the importance of invertible representations in GMs to predict crystal structures.

We note that, while GMs themselves offer essential architectures needed to inversely design materials with target

properties by navigating the functional latent space, many of the present examples shown above currently deal with generating new stable structures, and one still needs to incorporate properties into the model for a practical inverse design beyond stability embedding. One can use conditional GMs in which the target function is used as a condition,[68,85] or perform the optimization task on a continuous latent space as described in Gómez-Bombarelli et al.[21] for organic molecules. For example, Dong et al.[61] used a generative model to design graphene/boron nitride mixed lattice structures with the appropriate bandgap by adding a regression network within the GAN in combination with the simple lattice site representation. A similar crystal site-based representation[20] which satisfies both invertibility and invariance (Table 1) can be used to generate new elemental combinations for the fixed structure template. Also Kim et al.[60] used an image-based GAN model to inversely design zeolites with user-defined gas-adsorption properties by adding a penalty function that guides the target properties. Furthermore, Bhowmik et al.[86] provided a perspective on using a generative model for inverse design of complex battery interphases, and suggested that utilizing data taken from multiple domains (i.e. simulations and experiments) would be critical for the development of rationale generative models to enable accelerated discovery of durable ultra-high performance batteries.

3 Challenges and opportunities

Inorganic inverse design is an important key strategy to accelerate the discovery of novel inorganic functional materials, and various initial approaches have shown great promise as briefly summarized in the previous sections. To be used in more practical applications, there are several ongoing challenges. The grand challenge of inverse design is physical
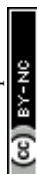
realization of newly predicted materials (*i.e.* reducing the gap between theory and experiment),[2] and the importance of developing an experimental feedback loop for newly discovered materials cannot be overemphasized. From the materials acceleration point of view, as mentioned in several previous reviews,[2,3,87] an experimental feedback loop can be significantly enhanced by robotic synthesis and characterization followed by AI making decisions for next experiments using Baysian optimization.[88–91] P. Nikolaev *et al.*[91] proposed an autonomous research system (ARES) which integrates autonomous robotics, artificial intelligence, data science (*i.e.* random forest model and genetic algorithm) and high-throughput/*in situ* techniques, and demonstrated its effectiveness for the case of carbon nanotube growth. More recently, MacLeod *et al.*[92] demonstrated a modular self-driving laboratory capable of autonomously synthesizing, processing, and characterizing organic thin films that maximize the hole mobility of organic hole transport materials for solar cell applications. These studies clearly show that the closed-loop approach can give unprecedented extension of our understanding and toolkits for novel materials discovery in an accelerated and automated fashion.

Another important missing ingredient is the lack of a model for synthesizability prediction for crystals. The screening and/or generation of hypothetical crystals produces a large number of promising candidates, but a significant number of them are not observed *via* experiments. Currently, hull energies (*i.e.* relative energy deviation from the ground state) are mostly used to evaluate the thermodynamic stability of crystals not because they are sufficient to predict synthesizability but mainly because they are simple quantities easily computable, but they are certainly insufficient to describe the complex phenomena of synthesizability of hypothetical materials.[93] Developing a reliable model or a descriptor for synthesizability prediction is thus an urgent and essential area for accelerated inverse design of inorganic solid-state materials.

In the case of GMs, as mentioned in the 'Generative models' section, developing an invertible and invariant model is still of great challenge since there is currently no explicit approach that simultaneously satisfies the latter two conditions. There are several promising data-driven approaches along this direction. Thomas *et al.*[94] proposed deep tensor field networks which have equivariance (*i.e.* generalized concept of invariance)[95] under rotational and translational transformation for 3D point clouds. A recently proposed deep learning model, AlphaFold,[96] predicting 3D protein structures from Euclidean distance geometry is also noteworthy since the distance between two atoms is an invariant quantity. Developing such invariant models and/or incorporating invariant features into 3D structures would thus be invaluable to develop more robust GMs for crystals.

Conflicts of interest

There are no conflicts of interest to declare.

Acknowledgements

References

1 K. Alberi, M. B. Nardelli, A. Zakutayev, L. Mitas, S. Curtarolo, A. Jain, M. Fornari, N. Marzari, I. Takeuchi and M. L. Green, *J. Phys. D: Appl. Phys.*, 2018, **52**, 013001.

2 A. Zunger, *Nat. Chem.*, 2018, **2**, 0121.

3 B. Sanchez-Lengeling and A. Aspuru-Guzik, *Science*, 2018, **361**, 360–365.

4 D. C. Elton, Z. Boukouvalas, M. D. Fuge and P. W. Chung, *Mol. Syst. Des. Eng.*, 2019, **4**, 828–849.

5 K. T. Butler, J. M. Frost, J. M. Skelton, K. L. Svane and A. Walsh, *Chem. Soc. Rev.*, 2016, **45**, 6138–6146.

6 E. O. Pyzer-Knapp, C. Suh, R. Gómez-Bombarelli, J. Aguilera-Iparraguirre and A. Aspuru-Guzik, *Annu. Rev. Mater. Res.*, 2015, **45**, 195–216.

7 A. R. Oganov, A. O. Lyakhov and M. Valle, *Acc. Chem. Res.*, 2011, **44**, 227–237.

8 A. Ludwig, *npj Comput. Mater.*, 2019, **5**, 70.

9 A. D. Sendek, Q. Yang, E. D. Cubuk, K.-A. N. Duerloo, Y. Cui and E. J. Reed, *Energy Environ. Sci.*, 2017, **10**, 306–320.

10 A. Jain, S. P. Ong, G. Hautier, W. Chen, W. D. Richards, S. Dacek, S. Cholia, D. Gunter, D. Skinner and G. Ceder, *APL Mater.*, 2013, **1**, 011002.

11 A. K. Singh, J. H. Montoya, J. M. Gregoire and K. A. Persson, *Nat. Commun.*, 2019, **10**, 1–9.

12 J. Noh, S. Kim, G. ho Gu, A. Shinde, L. Zhou, J. M. Gregoire and Y. Jung, *Chem. Commun.*, 2019, **55**, 13418–13421.

13 G. Hautier, C. C. Fischer, A. Jain, T. Mueller and G. Ceder, *Chem. Mater.*, 2010, **22**, 3762–3767.

14 K. Ryan, J. Lengyel and M. Shatruk, *J. Am. Chem. Soc.*, 2018, **140**, 10158–10168.

15 W. Sun, C. J. Bartel, E. Arca, S. R. Bauers, B. Matthews, B. Orvañanos, B.-R. Chen, M. F. Toney, L. T. Schelhas, W. Tumas, J. Tate, A. Zakutayev, S. Lany, A. M. Holder and G. Ceder, *Nat. Mater.*, 2019, **18**, 732–739.

16 A. Belsky, M. Hellenbrandt, V. L. Karen and P. Luksch, *Acta Crystallogr., Sect. B: Struct. Sci.*, 2002, **58**, 364–369.

17 R. Allmann and R. Hinek, *Acta Crystallogr., Sect. A: Found. Crystallogr.*, 2007, **63**, 412–417.

18 I. Tanaka, *Nanoinformatics*, Springer, 2018.

19 J. Schmidt, M. R. Marques, S. Botti and M. A. Marques, *npj Comput. Mater.*, 2019, **5**, 1–36.

20 F. A. Faber, A. Lindmaa, O. A. Von Lilienfeld and R. Armiento, *Phys. Rev. Lett.*, 2016, **117**, 135502.

21 R. Gómez-Bombarelli, J. N. Wei, D. Duvenaud, J. M. Hernández-Lobato, B. Sánchez-Lengeling, D. Sheberla, J. Aguilera-Iparraguirre, T. D. Hirzel, R. P. Adams and A. Aspuru-Guzik, *ACS Cent. Sci.*, 2018, **4**, 268–276.

22 B. Meredig, A. Agrawal, S. Kirklin, J. E. Saal, J. Doak, A. Thompson, K. Zhang, A. Choudhary and C. Wolverton, *Phys. Rev. B: Condens. Matter Mater. Phys.*, 2014, **89**, 094104.

23 A. Seko, H. Hayashi, K. Nakayama, A. Takahashi and I. Tanaka, *Phys. Rev. B: Condens. Matter Mater. Phys.*, 2017, **95**, 144110.

24 T. Xie and J. C. Grossman, *Phys. Rev. Lett.*, 2018, **120**, 145301.

25 C. W. Park and C. Wolverton, 2019, arXiv preprint arXiv:1906.05267.

26 C. Chen, W. Ye, Y. Zuo, C. Zheng and S. P. Ong, *Chem. Mater.*, 2019, **31**, 3564–3572.

27 J. Lym, G. H. Gu, Y. Jung and D. G. Vlachos, *J. Phys. Chem. C*, 2019, **123**, 18951–18959.

28 E. D. Cubuk, A. D. Sendek and E. J. Reed, *J. Chem. Phys.*, 2019, **150**, 214701.

29 M. H. Segler, T. Kogej, C. Tyrchan and M. P. Waller, *ACS Cent. Sci.*, 2018, **4**, 120–131.

30 H. Altae-Tran, B. Ramsundar, A. S. Pappu and V. Pande, *ACS Cent. Sci.*, 2017, **3**, 283–293.

31 B. Sánchez-Lengeling and A. Aspuru-Guzik, *ACS Cent. Sci.*, 2017, **3**, 275–277.

32 T. Mueller, A. Hernandez and C. Wang, *J. Chem. Phys.*, 2020, **152**, 050902.

33 V. L. Deringer, M. A. Caro and G. Csányi, *Adv. Mater.*, 2019, **31**, 1902765.

34 Y. Zuo, C. Chen, X. Li, Z. Deng, Y. Chen, J. r. Behler, G. Csányi, A. V. Shapeev, A. P. Thompson and M. A. Wood, *J. Phys. Chem. A*, 2020, **124**, 731–745.

35 J. Noh, G. H. Gu, S. Kim and Y. Jung, *J. Chem. Inf. Model.*, 2020, DOI: 10.1021/acs.jcim.0c00003.

36 S. Kim, J. Noh, G. H. Gu, A. Aspuru-Guzik and Y. Jung, 2020, arXiv:2004.01396.

37 A. R. Oganov, C. J. Pickard, Q. Zhu and R. J. Needs, *Nat. Rev. Mater.*, 2019, **4**, 331–348.

38 A. Franceschetti and A. Zunger, *Nature*, 1999, **402**, 60.

39 K. Doll, J. Schön and M. Jansen, *Phys. Rev. B: Condens. Matter Mater. Phys.*, 2008, **78**, 144110.

40 M. Amsler and S. Goedecker, *J. Chem. Phys.*, 2010, **133**, 224104.

41 F.-L. José, *J. Phys.: Condens. Matter*, 2020, DOI: 10.1088/1361-648X/ab7e54.

42 C. W. Glass, A. R. Oganov and N. Hansen, *Comput. Phys. Commun.*, 2006, **175**, 713–720.

43 Y. Wang, J. Lv, L. Zhu and Y. Ma, *Comput. Phys. Commun.*, 2012, **183**, 2063–2070.

44 I. A. Kruglov, A. G. Kvashnin, A. F. Goncharov, A. R. Oganov, S. S. Lobanov, N. Holtgrewe, S. Jiang, V. B. Prakapenka, E. Greenberg and A. V. Yanilkin, *Sci. Adv.*, 2018, **4**, eaat9776.

45 H. Zhu, J. Mao, Y. Li, J. Sun, Y. Wang, Q. Zhu, G. Li, Q. Song, J. Zhou and Y. Fu, *Nat. Commun.*, 2019, **10**, 270.

46 Y. Zhang, H. Wang, Y. Wang, L. Zhang and Y. Ma, *Phys. Rev. X*, 2017, **7**, 011017.

47 H. Xiang, B. Huang, E. Kan, S.-H. Wei and X. Gong, *Phys. Rev. Lett.*, 2013, **110**, 118702.

48 D. Bedghiou, F. H. Reguig and A. Boumaza, *Comput. Mater. Sci.*, 2019, **166**, 303–310.

49 E. V. Podryabinkin, E. V. Tikhonov, A. V. Shapeev and A. R. Oganov, *Phys. Rev. B: Condens. Matter Mater. Phys.*, 2019, **99**, 064114.

50 P. C. Jennings, S. Lysgaard, J. S. Hummelshøj, T. Vegge and T. Bligaard, *npj Comput. Mater.*, 2019, **5**, 1–6.

51 P. Avery, X. Wang, C. Oses, E. Gossett, D. M. Proserpio, C. Toher, S. Curtarolo and E. Zurek, *npj Comput. Mater.*, 2019, **5**, 1–11.

52 S. Curtarolo, W. Setyawan, G. L. Hart, M. Jahnatek, R. V. Chepulskii, R. H. Taylor, S. Wang, J. Xue, K. Yang and O. Levy, *Comput. Mater. Sci.*, 2012, **58**, 218–226.

53 A. Seko, H. Hayashi and I. Tanaka, *J. Chem. Phys.*, 2018, **148**, 241719.

54 A. Seko, H. Hayashi, H. Kashima and I. Tanaka, *Phys. Rev. Mater.*, 2018, **2**, 013805.

55 A. Halder, A. Ghosh and T. S. Dasgupta, *Phys. Rev. Mater.*, 2019, **3**, 084418.

56 A. Seko, T. Maekawa, K. Tsuda and I. Tanaka, *Phys. Rev. B: Condens. Matter Mater. Phys.*, 2014, **89**, 054303.

57 A. Mansouri Tehrani, A. O. Oliynyk, M. Parry, Z. Rizvi, S. Couper, F. Lin, L. Miyagi, T. D. Sparks and J. Brgoch, *J. Am. Chem. Soc.*, 2018, **140**, 9844–9853.

58 K. Kim, L. Ward, J. He, A. Krishna, A. Agrawal and C. Wolverton, *Phys. Rev. Mater.*, 2018, **2**, 123801.

59 J. Noh, J. Kim, H. S. Stein, B. Sanchez-Lengeling, J. M. Gregoire, A. Aspuru-Guzik and Y. Jung, *Matter*, 2019, **1**, 1370–1384.

60 B. Kim, S. Lee and J. Kim, *Sci. Adv.*, 2020, **6**, eaax9324.

61 Y. Dong, D. Li, C. Zhang, C. Wu, H. Wang, M. Xin, J. Cheng and J. Lin, 2019, arXiv preprint arXiv:1908.07959.

62 A. Nouira, N. Sokolovska and J.-C. Crivello, 2018, arXiv preprint arXiv:1810.11203.

63 D. Weininger, *J. Chem. Inf. Comput. Sci.*, 1988, **28**, 31–36.

64 M. Krenn, F. Häse, A. Nigam, P. Friederich and A. Aspuru-Guzik, 2019, arXiv preprint arXiv:1905.13741.

65 Y. Bengio, P. Simard and P. Frasconi, *IEEE Trans. Neural Netw.*, 1994, **5**, 157–166.

66 I. Sutskever, O. Vinyals and Q. V. Le, *presented in part at the Advances in neural information processing systems*, 2014.

67 A. Vaswani, N. Shazeer, N. Parmar, J. Uszkoreit, L. Jones, A. N. Gomez, Ł. Kaiser and I. Polosukhin, *presented in part at the Advances in neural information processing systems*, 2017.

68 Y. Li, L. Zhang and Z. Liu, *J. Cheminf.*, 2018, **10**, 33.

69 N. De Cao and T. Kipf, 2018, arXiv preprint arXiv:1805.11973.

70 D. Flam-Shepherd, T. Wu and A. Aspuru-Guzik, 2020, arXiv preprint arXiv:2002.07087.

71 F. Scarselli, M. Gori, A. C. Tsoi, M. Hagenbuchner and G. Monfardini, *IEEE Trans. Neural Netw.*, 2008, **20**, 61–80.

72 J. J. Irwin and B. K. Shoichet, *J. Chem. Inf. Model.*, 2005, **45**, 177–182.

73 D. P. Kingma and M. Welling, 2013, arXiv preprint arXiv:1312.6114.

74 I. Goodfellow, J. Pouget-Abadie, M. Mirza, B. Xu, D. Warde-Farley, S. Ozair, A. Courville and Y. Bengio, *presented in part at the Advances in neural information processing systems*, 2014.

75 K. Sohn, H. Lee and X. Yan, *presented in part at the Advances in neural information processing systems*, 2015.

76 M. Mirza and S. Osindero, 2014, arXiv preprint arXiv:1411.1784.

77 A. Makhzani, J. Shlens, N. Jaitly, I. Goodfellow and B. Frey, 2015, arXiv preprint arXiv:1511.05644.

78 A. B. L. Larsen, S. K. Sønderby, H. Larochelle and O. Winther, 2015, arXiv preprint arXiv:1512.09300.

79 J. Hoffmann, L. Maestrati, Y. Sawada, J. Tang, J. M. Sellier and Y. Bengio, 2019, arXiv preprint arXiv:1909.00949.

80 Ö. Çiçek, A. Abdulkadir, S. S. Lienkamp, T. Brox and O. Ronneberger, *presented in part at the Medical Image Computing and Computer-Assisted Intervention*, Cham, 2016.

81 S. Kajita, N. Ohba, R. Jinnouchi and R. Asahi, *Sci. Rep.*, 2017, **7**, 16991.

82 C. R. Qi, H. Su, K. Mo and L. J. Guibas, *presented in part at the Proceedings of the IEEE conference on computer vision and pattern recognition*, 2017.

83 Y. Sawada, K. Morikawa and M. Fujii, 2019, arXiv preprint arXiv:1910.11499.

84 Y. Dan, Y. Zhao, X. Li, S. Li, M. Hu and J. Hu, 2019, arXiv preprint arXiv:1911.05020.

85 S. Kang and K. Cho, *J. Chem. Inf. Model.*, 2018, **59**, 43–52.

86 A. Bhowmik, I. E. Castelli, J. M. Garcia-Lastra, P. B. Jørgensen, O. Winther and T. Vegge, *Energy Storage Mater.*, 2019, **21**, 446–456.

87 G. H. Gu, J. Noh, I. Kim and Y. Jung, *J. Mater. Chem. A*, 2019, **7**, 17096–17117.

88 P. S. Gromski, J. M. Granda and L. Cronin, *Trends Chem.*, 2019, **2**, 4–12.

89 F. Häse, L. M. Roch and A. Aspuru-Guzik, *Trends Chem.*, 2019, **1**, 282–291.

90 L. M. Roch, F. Häse, C. Kreisbeck, T. Tamayo-Mendoza, L. P. Yunker, J. E. Hein and A. Aspuru-Guzik, *Sci. Robot.*, 2018, **3**, eaat5559.

91 P. Nikolaev, D. Hooper, F. Webber, R. Rao, K. Decker, M. Krein, J. Poleski, R. Barto and B. Maruyama, *npj Comput. Mater.*, 2016, **2**, 16031.

92 B. P. MacLeod, F. G. Parlane, T. D. Morrissey, F. Häse, L. M. Roch, K. E. Dettelbach, R. Moreira, L. P. Yunker, M. B. Rooney and J. R. Deeth, 2019, arXiv preprint arXiv:1906.05398.

93 W. Sun, S. T. Dacek, S. P. Ong, G. Hautier, A. Jain, W. D. Richards, A. C. Gamst, K. A. Persson and G. Ceder, *Sci. Adv.*, 2016, **2**, e1600225.

94 N. Thomas, T. Smidt, S. Kearnes, L. Yang, L. Li, K. Kohlhoff and P. Riley, 2018, arXiv preprint arXiv:1802.08219.

95 D. Worrall and G. Brostow, *presented in part at the Proceedings of the European Conference on Computer Vision (ECCV)*, 2018.

96 A. W. Senior, R. Evans, J. Jumper, J. Kirkpatrick, L. Sifre, T. Green, C. Qin, A. Žídek, A. W. Nelson and A. Bridgland, *Nature*, 2020, 1–5.

97 C. J. Pickard and R. J. Needs, *Phys. Rev. Lett.*, 2006, **97**, 045504.

98 D. Grechishnikova, bioRxiv 863415, DOI: 10.1101/863415.